Supplementary Material

In Situ N-Doped Low-Corrosion Porous Carbon Derived from Biomass for Efficient CH_4/N_2 Separation

Huihui Wang [1], Yuqiong Zhao [1,*], He Lian [1], Qi Wang [2], Zhihong Shang [3] and Guojie Zhang [1,*]

[1] State Key Laboratory of Clean and Efficient Coal Utilization, Taiyuan University of Technology, Taiyuan 030024, China
[2] Department of Basic Sciences, Shanxi Agricultural University, Jinzhong 030801, China
[3] Jinneng Holding Group Co. Ltd., Taiyuan 030006, China
* Correspondence: zhaoyuqiong@tyut.edu.cn (Y.Z.), zhangguojie@tyut.edu.cn (G.Z.)

2.3 Characterization

The morphology of the porous carbon was examined using a scanning electron microscope (SEM; Gemini SEM 300). The extent of graphitization was assessed with an X-ray diffractometer (XRD; LabX-6000, Shimadzu, Japan) over a scanning range of 10-90° at a scan speed of 4 °/min. Fourier transform infrared spectroscopy (FTIR; Bruker TENSOR II, Germany) was employed to analyze the functional group variations in the material. X-ray photoelectron spectroscopy (XPS; Thermo Scientific ESCALAB 250Xi, USA) was used to investigate the surface elements of the porous carbon. The pore structure was characterized using a BSD-PS2 adsorption instrument. Before measurements, the samples were degassed under vacuum at 200 °C for more than six hours, and N_2 adsorption–desorption isotherms were recorded at 77K. The specific surface area was determined using the BET multi-point method, while the microporous volume and pore size distribution were evaluated through non-local density functional theory (NLDFT).

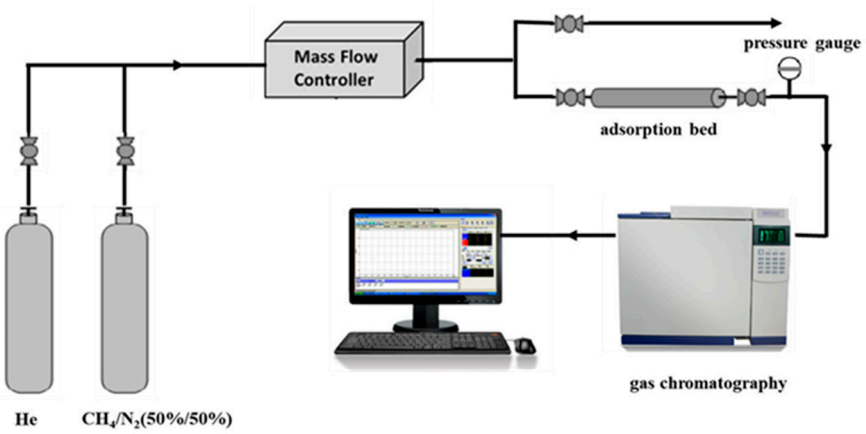


Figure S1. CH_4/N_2 breakthrough experimental equipment test diagrams.

Table S1. Carbon material yield.

Sample	M_1/g	M_2/g	Yield/%
S-800	5.00	1.75	35
Y-800	5.00	2.80	56
S_6Y_3-800	5.00	2.00	40
S_5Y_5-800	5.00	2.40	48
S_3Y_6-800	5.00	2.70	54
S_3Y_6-700	5.00	2.80	56

S_3Y_6-900	5.00	2.65	53
S_3Y_6-1000	5.00	2.60	52

M_1: Mass before activation

M_2: Mass after activation



Figure S2. Sample S_3Y_6-800.